Supplemental Material for Non-Arrhenius lithium diffusion with temperature-independent Haven ratio in garnet-type $Li_{6.5}La_3Zr_{1.5}Ta_{0.5}O_{12}$ single crystals

[1]Kaori Sugii, [1]Gen Hasegawa, [2]Kunimitsu Kataoka, [3]Kenjiro Hashi, [1]Junji Akimoto, [1]Kazunori Takada, [1,4]Naoaki Kuwata

[1] Research Center for Energy and Environmental Materials (GREEN), National Institute for Materials Science (NIMS), 1-1, Namiki, Tsukuba, Ibaraki 305-0044, Japan

[2] National Institute of Advanced Industrial Science and Technology (AIST), 1-1-1 Higashi, Tsukuba Ibaraki 305-8565, Japan

[3] Research Center for Advanced Measurement and Characterization, National Institute for Materials Science (NIMS), 3-13, Sakura, Tsukuba, Ibaraki 305-0003, Japan

[4] Graduate School of Chemical Science and Engineering, Hokkaido University, Kita 13, Nishi 8, Kita-ku, Sapporo, Hokkaido, Japan

I. Fitting using effective medium approximation (EMA) method

The non-Arrhenius conductivity of solid-state electrolytes will be explained by using the effective medium approximation (EMA). When two types of domains exist within a material, the total diffusion coefficient can be described using EMA. In LLZTO, we assume that two types of nano-domains exist: a low-temperature-dominant phase (LTP), in which the Li^+ ions are ordered, and a high-temperature-dominant phase (HTP), in which the Li ordering is dissolved. As the temperature rises, the area of HTP will gradually expand at intermediate temperatures. For simplicity, we assume that the volume fraction of HTP changes with temperature according to the Arrhenius relationship, $\frac{\varphi_{\mathrm{HTP}}}{\varphi_{\mathrm{LTP}}} = K_0 \exp\left(\frac{\Delta E}{k_B T}\right)$, where K_0 is a pre-exponential constant, ΔE is the activation

energy, k_B is the Boltzmann constant, and φ_{HTP}, φ_{LTP} are the volume fractions of HTP and LTP, respectively. The volume fractions obey a relation, $\varphi_{HTP} + \varphi_{LTP} = 1$. Using the Bruggeman-type EMA model, the diffusion coefficient is given by the following equation [39],

$$D_{EMA} = \frac{1}{4}\Big[(3\varphi_{HTP} - 1)D_{HTP} + (3\varphi_{LTP} - 1)D_{LTP} + \sqrt{\{(3\varphi_{HTP} - 1)D_{HTP} + (3\varphi_{LTP} - 1)D_{LTP}\}^2 + 8D_{HTP}D_{LTP}}\Big], \quad \text{(S1)}$$

where D_{HTP} and D_{LTP} are the diffusion coefficients of HTP and LTP, respectively. Both D_{HTP} and D_{LTP} obey the Arrhenius relationship, $D_{HTP} = D_{0,HTP}\exp(\Delta E_{HTP}/(k_B T))$ and $D_{LTP} = D_{0,LTP}\exp(\Delta E_{LTP}/(k_B T))$, where $D_{0,HTP}$ and $D_{0,LTP}$ are pre-exponential factors, and ΔE_{HTP} and ΔE_{LTP} are the activation energies of HTP and LTP, respectively. Now, we assume that ΔE_{LTP} is fixed to the experimental result at low temperatures (0.46 eV) and that ΔE_{HTP} equals to the high-temperature E_a (0.31 eV) determined by T_1 analysis.

The fitting results using EMA method ($D_{\sigma,EMA}$ and $D_{NMR,EMA}$) are shown in Fig. S6(a). Here, two diffusion coefficients are connected by a constant Haven ratio of 0.38, $H_R = D_{\sigma,EMA}/D_{NMR,EMA}$. The fitting parameters are $K_0 = 0.006$, $\Delta E = 0.21$ eV, $D_{0,HTP} = 3.9 \times 10^{-8}$ m^2 s^{-1}, and $D_{0,LTP} = 5.3 \times 10^{-6}$ m^2 s^{-1}. The assumption that the HTP area broadens with temperature could be considered aggressive because there is no empirical evidence to support it. However, the temperature variations of $D_{\sigma,EMA}$ and $D_{NMR,EMA}$ are in good agreement with the experimental results across a wide temperature range.

II. Fitting using bond strength-coordination number fluctuation (BSCNF) model

It is known that the temperature dependence of conductivity in glassy ionic conductors is similar to that of crystalline superionic conductors. Based on this similarity, Okada et al. have attempted to apply a common conduction mechanism to both glasses and crystals to explain the non-Arrhenius type ionic conductivity [13]. Assuming the BSCNF model, the bonding nature fluctuates between ionic and covalent as the ion migrates near the non-mobile atoms. Consequently, the bonding energy $\tilde{E}$ between the mobile ion and its surrounding ions fluctuates, as does the coordination number of the mobile ion $\tilde{Z}$. The ionic conductivity σ is given by

$$\sigma T = \frac{A_{\sigma T}\sqrt{T^2 - \left(\Delta\tilde{E}\Delta\tilde{Z}/R\right)^2}}{T} \exp\left(-\frac{\tilde{E}_0\tilde{Z}_0/R}{T - \Delta\tilde{E}\Delta\tilde{Z}/R}\right). \quad \text{(S2)}$$

Here, $\tilde{E}_0$ is mean value of the bond energy between the mobile and the surrounding ions, $\tilde{Z}_0$ is the mean value of the coordination number of the mobile ion, and $\Delta\tilde{E}$ and $\Delta\tilde{Z}$ are their fluctuations. R is the gas constant, and $A_{\sigma T}$ is a constant. According to fitting results in Ref. [13], $\tilde{E}_0\tilde{Z}_0/R$ ranges from 650 to 8000 K, and $\Delta\tilde{E}\Delta\tilde{Z}/R$ ranges from 10 to 365 K. For LLZTO single crystal, the same fitting was performed, resulting in following parameters: $\tilde{E}_0\tilde{Z}_0/R$ = 2661 K and $\Delta\tilde{E}\Delta\tilde{Z}/R$ = 82 K. The fitting results is presented in Fig. S6(b). We also convert the calculated σ into the diffusion coefficients ($D_{\sigma,\mathrm{BSCNF}}$ and $D_{\mathrm{NMR,BSCNF}}$) using Eq. (3) and a constant H_R. The fitting results are shown in Fig. S5(b). As is the case with numerous ionic conductors, including lithium solid-state electrolytes, the fitting curve using Eq. (S2) well explains the ionic conductivity of LLZTO.

III. Correlation factors

The single-particle correlation factor f and collective correlation factor f_I are defined as

$$f = D_\mathrm{NMR}/D_{\text{local jump}}, \quad \text{(S3)}$$

$$f_\mathrm{I} = D_\sigma/D_{\text{local jump}}, \quad \text{(S4)}$$

respectively, where $D_{\text{local jump}}$ represents the diffusion coefficient expected from local, uncorrelated jumps. The Haven ratio [20,39,50] is then expressed as

$$H_R = f/f_\mathrm{I}. \quad \text{(S5)}$$

Here, $D_{\text{local jump}}$ can be roughly estimated from the correlation time at the T_1 minimum using the relation

$$D_{\text{local jump}} = D_{\mathrm{local,T1}} = {l_\mathrm{hop}}^2/2d\tau_\mathrm{c}, \quad \text{(S6)}$$

assuming an isotropic three-dimensional random walk. The $D_{\mathrm{local,T1}}$ is plotted in Fig. 5(c). The estimated $D_{\mathrm{local,T1}}$ lies between D_NMR and D_σ, yielding f = 0.7 and f_I = 2.1.

The value of f_I exceeding unity does not conform to the expectation for a simple uncorrelated random-jump model [20]. This discrepancy most likely arises from the simplified estimation of $D_{\text{local jump}}$. In particular, the correlation time obtained from the T_1 analysis may not correspond directly to the mean residence time between successful long-range jumps, and the estimated

$D_{\text{local jump}}$ depends on the assumed jump distance, dimensionality, jump geometry, and the validity of the BPP-type model. Furthermore, because the temperature dependence of T_1 requires more than one motional contribution, the correlation time at the T_1 minimum should be regarded as an effective value.

The result also indicates that the $D_{\text{local,T1}}$ value derived from the T_1 minimum cannot be regarded as an unambiguous uncorrelated reference diffusivity. This discrepancy may arise because the T_1-derived $D_{\text{local,T1}}$, D_{NMR}, and D_σ probe ionic motion over different time and length scales and are based on different model assumptions. Therefore, the individual values of f and f_1 should be interpreted with caution, although their ratio remains consistent with the experimentally determined Haven ratio.

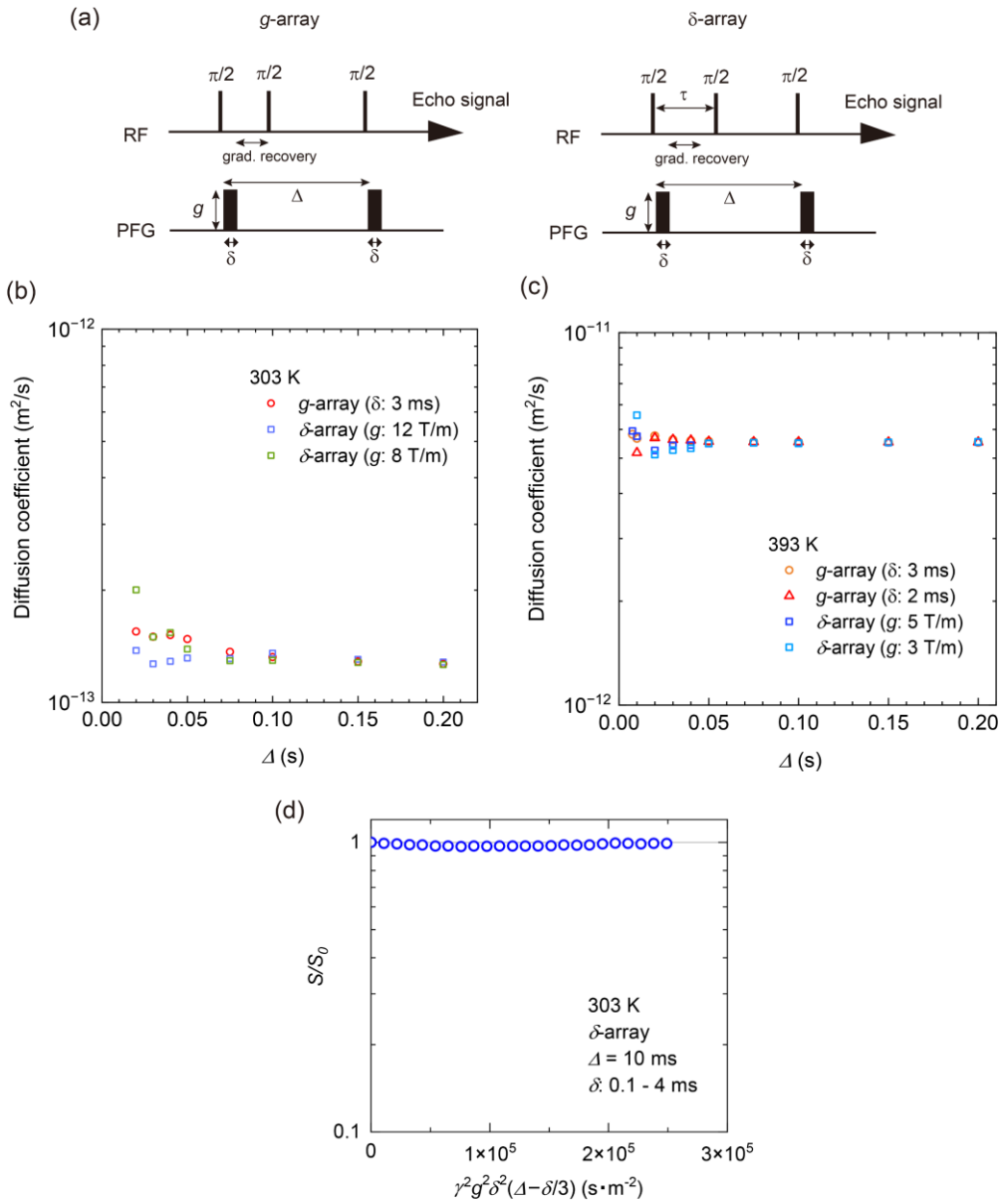


FIG. S1. (a) Two kinds of PFG-NMR pulse sequences [21]. In the *g*-array (left) sequence, the gradient field strength *g* is changed while the gradient field pulse width δ is constant. In the δ-array (right) sequence, δ is changed while *g* is unchanged. (b) Δ dependence of diffusion coefficient using *g*- and δ-array sequences at 303 K. (c) Δ dependence of diffusion coefficient using *g*- and δ-array sequences at 393 K. (d) Echo attenuation plot at 303K, using δ-array sequence. No significant attenuation is observed at Δ = 10 ms. These results differ considerably from the prior findings reported by Hayamizu et al. [37].

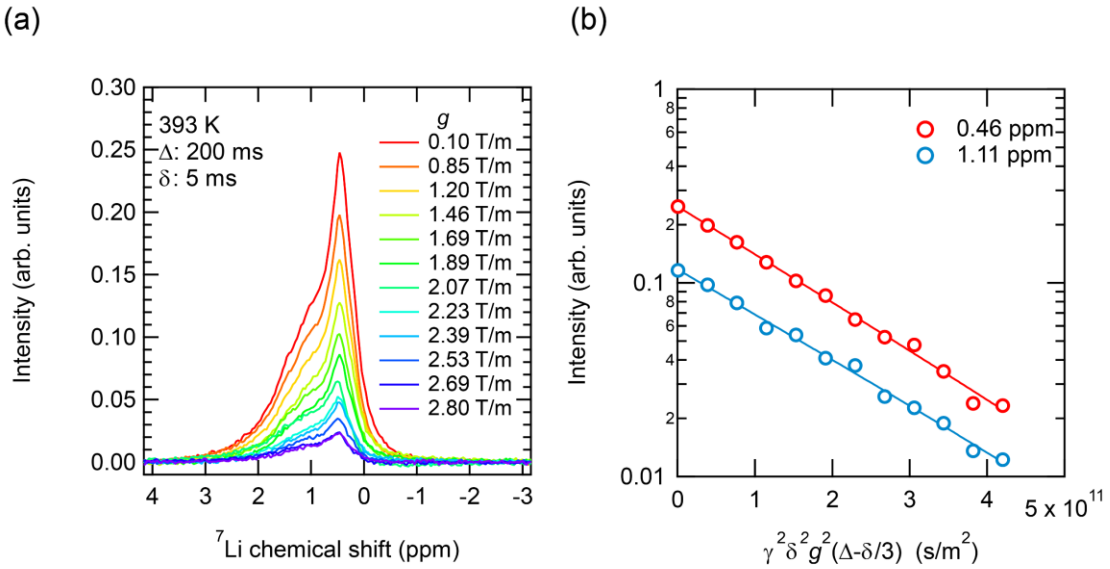


FIG. S2. (a) Attenuation of NMR echo signals when g varies from 0.1 to 2.8 Tm^{-1} at 393 K. Δ is 200 ms and δ is 5 ms. (b) Echo attenuation plots at two different chemical shifts at 0.46 (red) and 1.11 ppm (blue). The echo intensities are fitted by the Stejskal−Tanner equation denoted by the solid lines. Resultant diffusion coefficients are 5.7 × 10^{-12} m^2 s^{-1} (at 0.46 ppm) and 5.3 × 10^{-12} m^2 s^{-1} (at 1.11 ppm), respectively. Even if the diffusion coefficient is estimated from the decay curve at any given point, the variation is negligible.

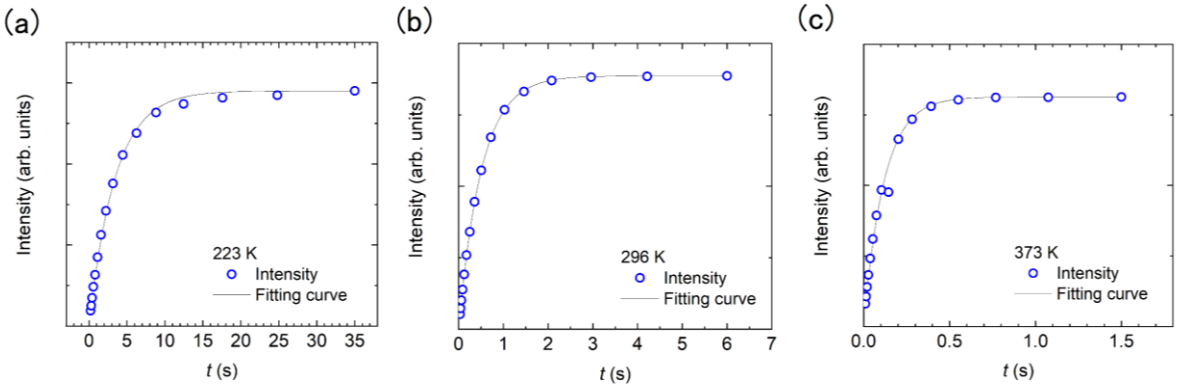


FIG S3. Saturation recovery curves in T_1 measurements at (a) 223 K, (b) 296 K, and (c) 373 K, respectively. The solid black lines represent fits using a single-exponential recovery function.

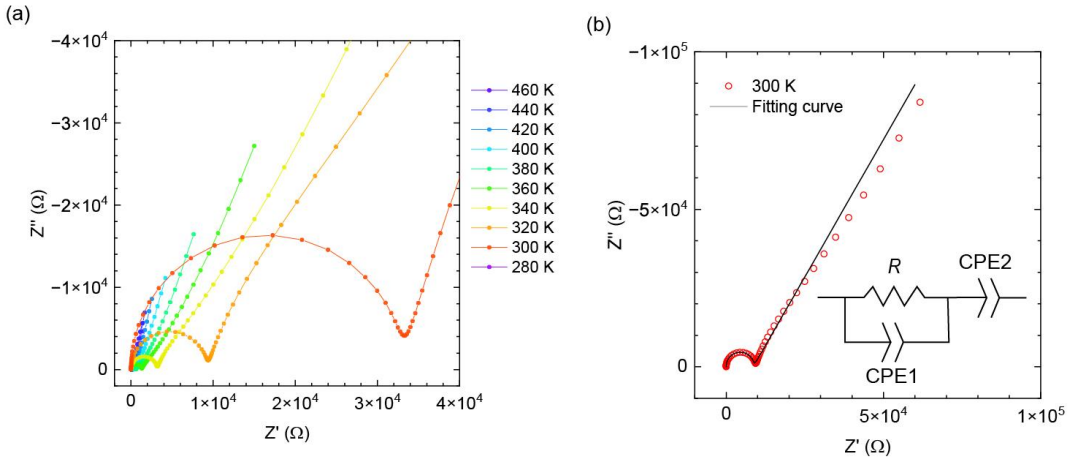


FIG. S4. (a) Nyquist plots of LLZTO at various temperatures from 280 to 460 K. (b) Nyquist plot of LLZTO at 300 K. Solid black line is the fitting calculated using equivalent circuit consisting of constant phase element (CPE) and resistance (R). A parallel R-CPE1 element corresponds to the bulk impedance and CPE2 corresponds to the electrode interface impedance.

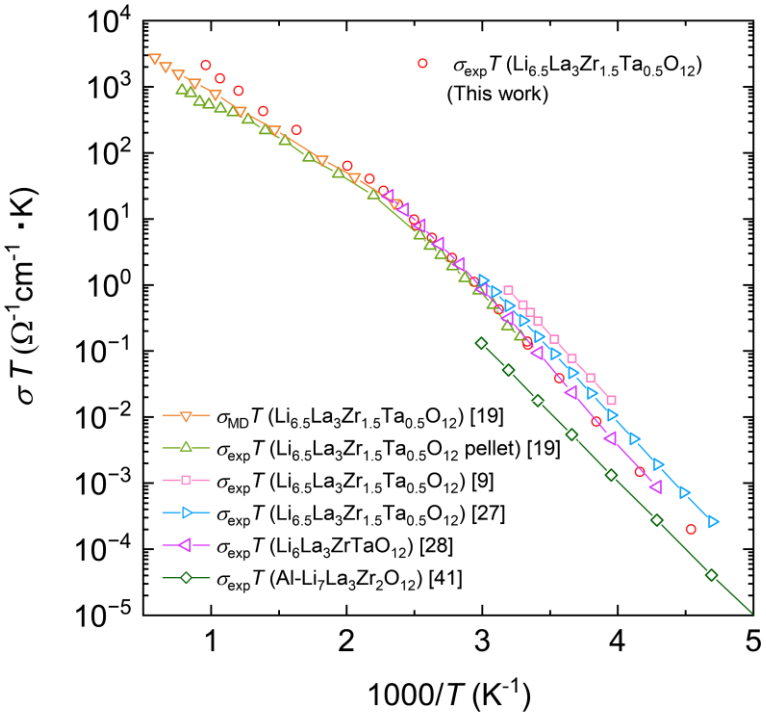


FIG. S5. σT vs $1000/T$ plots of cubic garnet-type electrolytes. The ionic conductivities of single crystals of $Li_{6.5}La_3Zr_{1.5}Ta_{0.5}O_{12}$ [9,27] and $Li_6La_3ZrTaO_{12}$ [28] in prior researches are presented. The ionic conductivities of pellet $Li_{6.5}La_3Zr_{1.5}Ta_{0.5}O_{12}$ [19], Al-contained $Li_7La_3Zr_2O_{12}$ [41], and MD simulation [19] are also shown.

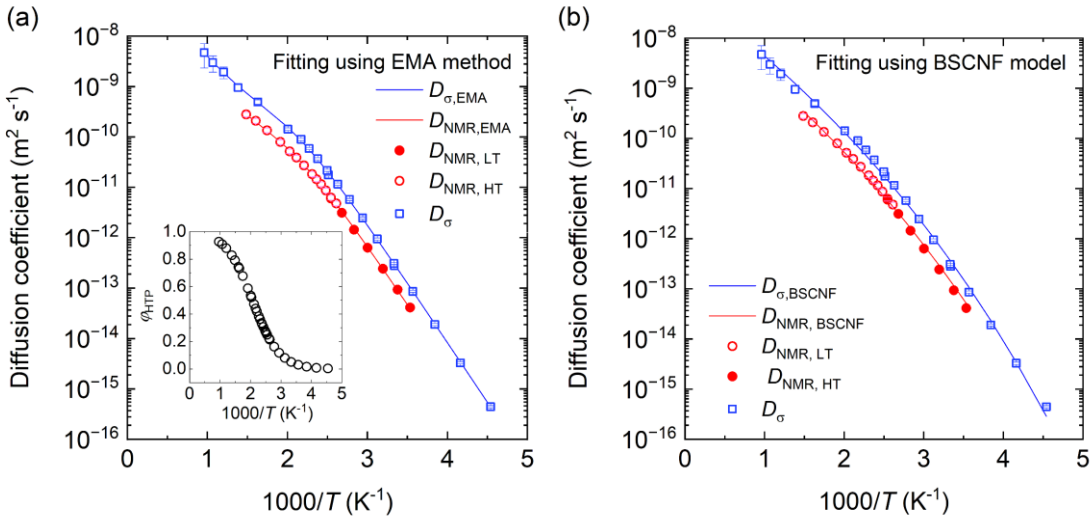


FIG. S6. Fitted D_{NMR} and D_{σ} by using (a) the EMA method and (b) the BSCNF model. Inset of (a) shows the temperature variation of the volume fraction of the high-temperature phase, φ_{HTP}.